Journal of Applied Polymer Science

Thermoresponsive Hydrogels from BSA Esterified with Low Molecular Weight PEG

Kai Wang,[1] Gisela Buschle-Diller,[1] Yonnie Wu[2]
[1]Department of Polymer and Fiber Engineering, Auburn University, Auburn, Alabama 36849-5327
[2]Department of Chemistry and Biochemistry, Auburn University, Auburn, Alabama 36849-5312
Correspondence to: G. Buschle-Diller (E-mail: buschgi@auburn.edu)

ABSTRACT: Bovine serum albumin (BSA) and low molecular weight polyethylene glycol (PEG) were reacted in a single-step reaction to synthesize translucent hydrogels with a sol–gel transition at temperatures between 37 and 40°C. Gelation occurred by aggregation of smaller assemblies of BSA–PEG precursors within minutes. The sol–gel transition concentration depended on the molecular weight of PEG only at temperatures below 35°C; above 45°C phase separation occurred and a precipitate formed. Microscopic examination showed the porous structure of the gels. At a fairly low grafting ratio, BSA preserved its native secondary and tertiary structure and maintained its capability for binding and enclosing small molecules. Drug delivery was assessed by a discontinuous method *in vitro* using 5-fluorouracil. Degradation tests with trypsin confirmed that the hydrogels were biodegradable. This novel material holds promise for biomedical applications as potentially injectable drug delivery vehicle. © 2014 Wiley Periodicals, Inc. J. Appl. Polym. Sci. **2014**, *131*, 40946.

KEYWORDS: biomaterials; drug delivery systems; gels; proteins

Received 4 March 2014; accepted 1 May 2014
DOI: 10.1002/app.40946

INTRODUCTION

Biopolymeric thermoresponsive gels with a sol–gel transition at body temperature have been the recent focus of biomedical research.[1] These gels have a great potential for drug delivery reservoirs while being injectable at a specific location of need.[2–6] It is a challenging task to create such a gel that additionally fulfills nontoxicity requirements, disintegrates without cytotoxicity of the resulting products in a controlled manner and releases drugs within a useful time frame.

In general, hydrogels can be defined as materials that form three-dimensional molecular networks capable of holding large amounts of water. They are considered thermoresponsive when a temperature change functions as the stimulus to perform a desired task, e.g., swelling and collapse.[7] Stimuli-sensitive hydrogels have found extensive interest as drug delivery vehicles.[8] The most recent focus of research has been directed towards hydrogels for which the aqueous precursor is a fluid at room temperature and a gel at body temperature. This behavior could make it possible to form a hydrogel *in situ* upon injection via *in vivo* crosslinking[9] or by other mechanisms[1]—as opposed to a preformed hydrogel—and therefore well adjust to a required defect geometry. For biomedical applications as for tissue repair, it is adamant that the gelation to be conducted under mild conditions and without the use of toxic chemicals, and that the generation of excessive heat or the release of gaseous by-products to be avoided as it could adversely affect tissue. Suitable materials also require biocompatibility, biodegradability, and homogeneous dispensation of loaded drugs or cells.

For thermoresponsive hydrogels, both natural and synthetic polymers have been explored. Among synthetic polymers, a fairly large number of poly(*N*-isopropyl acrylamide) (poly(NIPAAM))-based systems have been investigated for their sol–gel behavior[10,11] and efforts have been reported to adjust their lower critical solution temperature (LCST) to the physiologically interesting range by modification of the gel architecture, crosslinking and/or copolymerization with natural or synthetic compounds.[12,13] Block copolymeric networks have also been formed based on polyesters, for instance, polylactide (PLA) and polylactide-co-glycolide (PLGA),[14–16] frequently with poly(ethylene glycol) (PEG) as a copolymer.[17–20] Synthetic injectable hydrogels, however, may cause more severe immunologic reactions than natural polymer based materials and show a lower degradability rate.[21,22]

As natural polymers, polysaccharide-based hydrogels have been studied such as chitosan, xylan, hyaluronic acid, and alginate,[23,24] as well as protein [gelatin, collagen, fibrinogen, and bovine serum albumin (BSA)][21,22,25] and synthetic polypeptide-based ones (e.g., poly(L-glutamates[20]). Direct reaction of PEG

or PEG derivatives (aldehydes, carboxylates, carbonates, and thiols) with the base polymer have also frequently been used in an attempt to adjust the LCST closer to the desired range.[26–33] The addition of PEG increases the hydrophilicity of the base polymers and their overall molecular weight. PEG with higher molecular weight increases the repulsion of the modified BSA to the phospholipids of the cell membrane, thus, lowering the interaction with cells.[19,21,29,33]

Some of the synthetic thermoresponsive hydrogel products have already been approved by FDA for medical applications (e.g., Pluronic™, ReGel™)[3,5,34,35] and most of them can be degraded by metabolic enzymes.[34] However, the complexity of the reaction, the toxicity of some of the reactants, and the low solubility of hydrophobic drugs in the hydrogel still present significant drawbacks.[29–33] Polypeptide or protein-based PEGylated hydrogels generally exhibit superior performance in drug delivery and tissue engineering.[20]

The motivation for this research was to develop a simplified approach to create a PEG-grafted BSA hydrogel, using low-molecular weight PEG simultaneously as a reactant and dispersion medium. The desired sol–gel transition of this hydrogel should be in the range of the body temperature so that the hydrogel could potentially be injected. It was assessed whether the chain length of PEG with molecular weight 200 or 400, directly grafted via esterification of the acidic BSA residues, could have a distinct effect on the sol–gel transition. Finally, the attempt was made to preserve the secondary/tertiary structure of BSA during and after the reaction, so that the resultant BSA–PEG would be able to hold small molecules for potential drug delivery. Such a thermoresponsive hydrogel could serve as a drug carrier as well as a model compound for other protein-based hydrogels.

EXPERIMENTAL

Materials and Chemicals

BSA was purchased from Sigma-Aldrich; PEG200, PEG400, diethyl ether, and ethanol were obtained from Alfa Aesar and 98% sulfuric acid from EMD. 5-FU (5-fluorouracil) was also purchased from Sigma-Aldrich. Trypsin (1 : 250, tissue culture grade) and phosphate buffered saline (PBS) were obtained from Amresco.

Preparation of BSA–PEG Precursor

The procedure used to make the hydrogel precursors was roughly adapted from Chen et al.[20] : 0.5 g BSA were suspended in 20 mL PEG (molecular weights 200 and 400, respectively), and 0.5 mL sulfuric acid (98%) was added dropwise. The reaction was conducted overnight at room temperature. The product was separated by precipitation in a 1 : 1 mixture of ethanol and diethyl ether and centrifuged at 5000 rpm for 10 min. The obtained solid product was dissolved in 20 mL 50 m*M* phosphate buffer saline (PBS) at pH 7.4, and separated from trace amounts of unreacted PEG by centrifugal ultrafiltration (Amicon Ultra-15, MWCO 30 KDa, EMD Millipore). Ultrafiltration was repeated three more times with deionized (DI) water. The obtained BSA–PEG precursor was prefrozen at −18°C and dried by lyophilization. The yield of purified product was 76.9% for BSA–PEG200 (0.4 g) and 57.3% for BSA–PEG400 (0.32 g).

Gelation

For the gelation experiments 0.5 g BSA–PEG precursor (PEG molecular weights 200 and 400, respectively) was dissolved in 10 mL 50 m*M* PBS (pH 7.4) and the solution brought to a concentration of 15% (wt) (3.3 g) using centrifugal ultrafiltration at 5000 rpm. Precursor solution was filled in individual vials and heated in a water bath to various temperatures (25, 30, 35, 37, and 40°C) for 30 min. If gelation did not occur under these conditions, the concentration was increased until the precursor gelled and the mass was determined by weighing the sample vials. The sol–gel transition concentration of the formed hydrogel was calculated by the following equation (eq. (1))

$$W = \frac{m'}{m} \times 100\% \quad (1)$$

The mass (g) of the hydrogel at gelation is m, and m' is the mass of hydrogel precursor (0.5 g); W is the hydrogel precursor weight percentage at sol–gel transition.

A tubular polyacrylamide mold of 10 mm inner diameter and 4 mm depth was prepared into which the precursor gel was injected. The mold was preheated to a set temperature for the gelation experiments and the gelling ability of the precursor studied under these conditions.

Drug Delivery

Drug loading capacity of BSA–PEG200 and BSA–PEG400 solution, respectively, was evaluated by the following method: 1 mg mL^{-1} 5-FU solution in 50 m*M* PBS at pH 7.4 was mixed with different molar ratios of BSA to 5-FU (100, 200, 300, and 400). BSA–PEG and 5-FU were incubated at 40°C for 2 h, and separated by ultrafiltration (Amicon Ultra-15, MWCO 30 KDa, EMD Millipore).[36] Separated 5-FU solution concentration was used to determine the drug loading ratio by the following equation (eq. (2)):

$$R = R' \times \frac{C_i - C_f}{C_i} \quad (2)$$

Here, R is the loaded 5-FU to BSA molar ratio, C_i is the initial 5-FU concentration (1 mg mL^{-1}) and C_f is the concentration of separated 5-FU determined by UV–vis, R' is the incubated-BSA to 5-FU molar ratio. Release of 5-FU was determined by a discontinuous method.[17] Each type of hydrogel (0.5 g) was sealed in an individual dialysis tube (MWCO 30 kDa) and exposed to 50 mL 50 m*M* PBS at pH 7.4, with native BSA gelled at 70°C as the control sample. For UV–vis spectroscopic examination, 4 mL of the solution were used and 4 mL 50 m*M* fresh PBS were added to maintain the total volume.

Degradation

Degradation experiments were performed with 15% BSA–PEG200 and BSA–PEG400 hydrogels, respectively. Each sample contained 1 g hydrogel enclosed in 20 mL vials and heated to 40°C; 10 mL 0.05*M* PBS (pH adjusted to 8) with 10 U mL^{-1} trypsin were added to the vials. The control sample only contained hydrogels in 10 mL 0.05*M* PBS (no trypsin). The vials were kept in 37°C in a water bath and stirred. Vials were

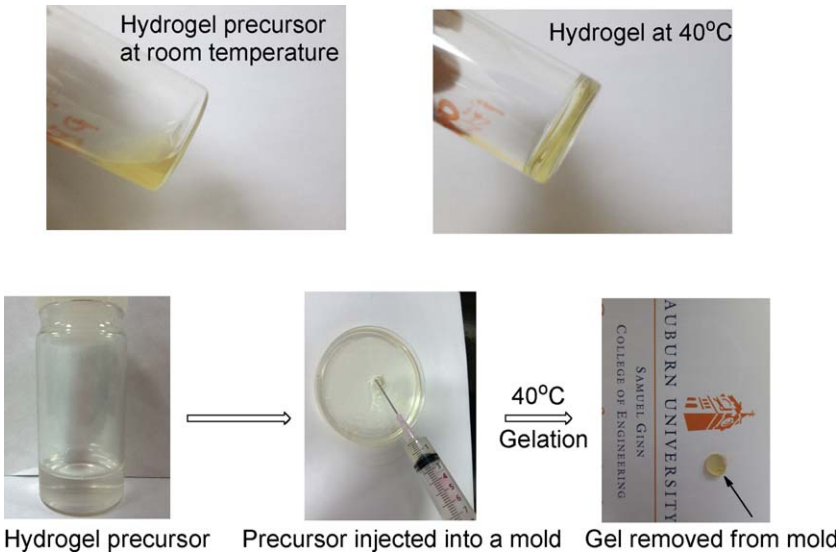

Figure 1. Precursor (in 0.05 *M* PBS, pH = 7.4) was liquid at room temperature and a hydrogel was obtained with heating to 40°C. [Color figure can be viewed in the online issue, which is available at wileyonlinelibrary.com.]

weighed before the degradation process was started. After every 12 h, 10 mL solution was removed from the vials and the same volume (10 mL) PBS added. The vials were weighed at every interval. The degradation test was conducted for 7 days.

Characterization

Fourier Transform Infrared spectroscopy (FT-IR) was conducted using a Thermo Scientific Nicolet 6700 FT-IR spectrometer for the chemical characterization of the products; the wave number range was set at 4000–400 cm^{-1} over 32 scans with a resolution of 4 cm^{-1}. IR (ATR): v = 3270 (m), 2939 (w), 2890 (w), 1623 (s, amine I), 1540 (m, amine II) 1187 (s, C—N), 1083 (s, C—O) cm^{-1}.

A Bruker Microflex LT MALDI-TOF mass spectrometer and control software from Bruker Daltonics were utilized to estimate the molecular weight. The range for the MALDI-TOF test was 20–250 kDa. Sinapic acid and native BSA protein were used as matrix.

^{1}H-NMR spectroscopy was conducted on a Bruker 400MHz spectrometer to determine the molecular structure and estimate the PEGylation ratio. Samples were dissolved in 0.5 mL deuterium oxide and water was used as reference. ^{1}H-NMR (400 MHz, D_2O, δ): 7.20 (m, 2H; ArH), 4.70 (m, 1H, CH), 3.59 (m, 4H; OCH_2CH_2), 2.87 (m, 2H; NH_2), 1.53 (m, 2H; CH_2), 0.75 (m, 3H; CH_3) ppm.

UV–vis was carried out on a Thermo Scientific Genesys 6 spectrometer to quantify the 5-FU to BSA ratio. Quartz cuvettes with 10 mm path length were used. UV–vis (0.05*M* PBS, pH = 7.4): $\lambda_{max}(\varepsilon)$ = 280 (3,443,824 M^{-1} cm^{-1}, BSA), 266 nm (7070, $M^{-1}cm^{-1}$, 5-FU).

Circular dichroism (CD) spectra were obtained by using a JASCO-810 spectropolarimeter (Jasco, Tokyo, Japan) with collecting wavelength ranges from 180 to 300 nm to investigate the secondary and tertiary structure of hydrogel protein moieties. Quartz cuvettes with 0.2 mm path length were used, and the average molecular weight of BSA residues was considered to be 114 g mol^{-1}.[37,38] Samples were dissolved in 0.05 *M* PBS at pH 7.4 with a concentration of 1 mg mL^{-1}. Protein moiety ellipticity was determined by eq. (3):

$$\theta = 114\theta_\lambda / 10dc \quad (3)$$

where θ_λ is the observed ellipticity, d is the light path and c the concentration. Prior to CD analysis, SDS-PAGE was used to confirm the presence of protein; UV–vis evaluations were performed to determine the solution concentration.

A Carl Zeiss EVO 50 scanning electron microscope (SEM) at 20 kV scanning voltage was used to examine the morphology of dried hydrogels. Gold coating was applied by a sputter coater prior to imaging. The hydrogels were frozen in liquid nitrogen and dried in a freeze dryer. A Carl Zeiss EM 10 transmission electron microscope (TEM) at 60 kV scanning voltage was used for observation of aggregate sizes. 10 μL 1 and 15% BSA–PEG solutions were placed on a 300 mesh copper grid on filter paper to prepare a thin film. The copper grid was frozen with liquid nitrogen and dried in a freeze dryer.

Rheology tests were performed on a TA Instrument AR2000 Rheometer with a 60 mm diameter flat plate at 0.05 mm gauge by frequency sweeping oscillatory method with 0.1 to 100 Hz frequency. Both the 15% hydrogel precursors and the resultant hydrogels were tested at optimized gelation temperature.

RESULTS AND DISCUSSION

PEGylation of BSA

BSA and liquid, low molecular weight PEG was reacted with sulfuric acid as the catalyst to form a translucent hydrogel precursor. At room temperature the product precursors showed excellent solubility in both DI water and PBS of pH 7.4 (Figure 1), irrespective of the molecular weight of PEG (200 or 400)

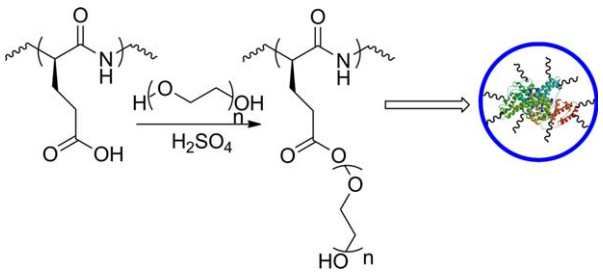

Figure 2. Schematic of the synthesis and formation of a potentially injectable hydrogel: precursor synthesized from BSA and PEG. [Color figure can be viewed in the online issue, which is available at wileyonlinelibrary.com.]

and the grafting ratio. Successful grafting was verified by FT-IR with the 1083 cm^{-1} absorption peak of the repeat units of PEG.

PEG reacted with a fraction of the 96 acidic residues of BSA [glutamic acid (Glu) and aspartic acid (Asp)] by formation of covalent bonds via a single-step reaction. This reaction constitutes an esterification in which PEG can serve as both the reactant and the dispersion medium for BSA. Grafting low molecular weight PEG contributes to product solubility by adding ethylene oxide units to the protein. Further, the hydrophilicity of BSA is considerably impacted because each ethylene oxide group could theoretically trap three water molecules.[26] With PEGylation of the BSA protein the formation of aggregates becomes possible through short, more hydrophilic PEG tails oriented towards water and away from the relatively hydrophobic BSA moiety in different arrangements (Figure 2).

The average molecular weight and grafting ratio of BSA–PEG were determined from the mass spectra (Figure 3). As shown in Table I, the average molecular weight of BSA–PEG200 was 69.1 kDa, and for BSA–PEG400 73.7 kDa. There were an average of 13 mole PEG200 and 18 mole PEG400 grafted to each mole BSA involving approximately one-fifth of its acidic residues

Table I. Molecular Weight of BSA–PEG200 and BSA–PEG400 Determined from MALTI-TOF Mass Spectra

Sample	Mn (kDa)	Standard deviation (kDa)	Grafting ratio
BSA-PEG200	69.1	2.53	13
BSA-PEG400	73.7	1.26	18

(Asp and Glu, see H^1-NMR spectra in Figure 5). The mass spectra did not indicate the formation of any significant amounts of BSA dimers, trimers or oligomers nor any major damage to BSA from the acid catalysis during the PEGylation reaction.

The CD spectra of the samples, with native BSA as the control, showed the characteristic peaks at 210 and 225 nm that indicate alpha-helical structure which was predominant in the secondary and tertiary structure of the native protein. The ellipticity of all the samples was in the same range (Figure 4), which revealed that the secondary and tertiary structure of BSA was indeed preserved throughout the reaction. This result was also confirmed by FT-IR spectra. The band at 1623 cm^{-1} for the amino group absorption remained unchanged. Only a limited number of BSA amino acid residues were esterified under the experimental conditions (Table I), while others remained unreacted. Thus, the majority of native secondary structure of BSA was not affected by the PEGylation reaction.

The proton NMR spectra in Figure 5 support that PEG grafting has been accomplished by exhibiting a strong peak for ethoxyl groups at δ 3.59. The PEG grafting ratio can be approximated by integrating the peak intensity ratios of the aromatic groups (δ7.15) to ethoxyl groups. As mentioned above, the PEG200 and PEG400 only reacted with acidic residues (Asp and Glu) of BSA, which is reflected by unaffected amino groups (Lys, Asn, and Gln). The integrated peak intensity ratio of acidic residues

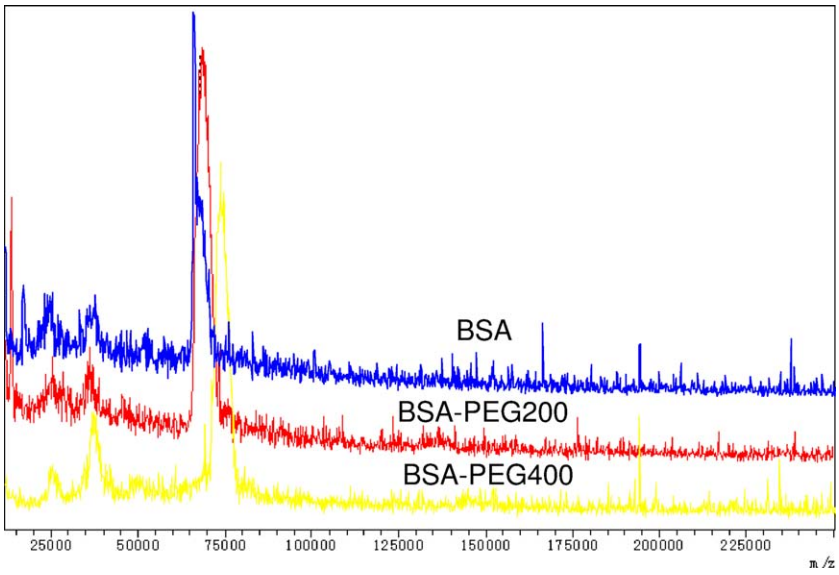

Figure 3. MALDI-TOF mass spectra of BSA, BSA–PEG200, and BSA–PEG400. [Color figure can be viewed in the online issue, which is available at wileyonlinelibrary.com.]

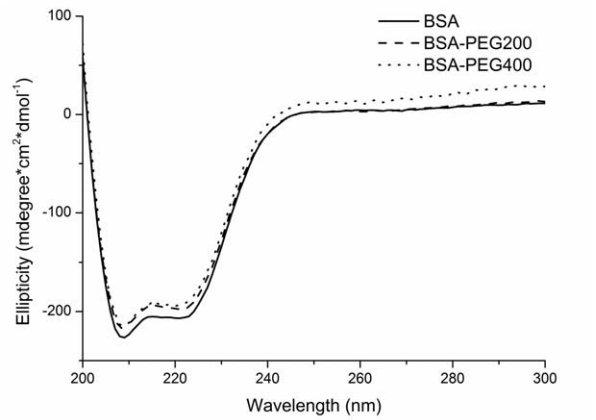

Figure 4. CD spectra of the BSA as control, BSA–PEG200 and BSA–PEG400 dissolved in 0.05*M* PBS at pH 7.4.

to aromatic groups resulted in similar PEGylation ratios as obtained from mass spectra (Figure 3).

Sol–Gel Behavior

The lower critical solution temperature (LCST) determines the solubility of a polymer (hydrogel) in a solvent (water) and thus its sol–gel behavior. The gelation of unmodified BSA at physiological pH occurs at around 80°C.[39] If polypeptides are reacted with PEG, the LCST can be lowered and the length of the PEG chains and the ratio of PEG grafting may have an effect on the LCST.[12,20,40]

As shown in Figure 1, synthesized hydrogel precursors were liquid at room temperature, and the gelation of condensed hydrogel precursors occurred when heated up to 40°C. When injected into a preheated polyacrylamide mold, soft yellowish gels could be formed that completely filled the shape of the mold within minutes.

Although PEG grafting only occurred at a limited number of residues in BSA and the molecular weight of PEG was low, it

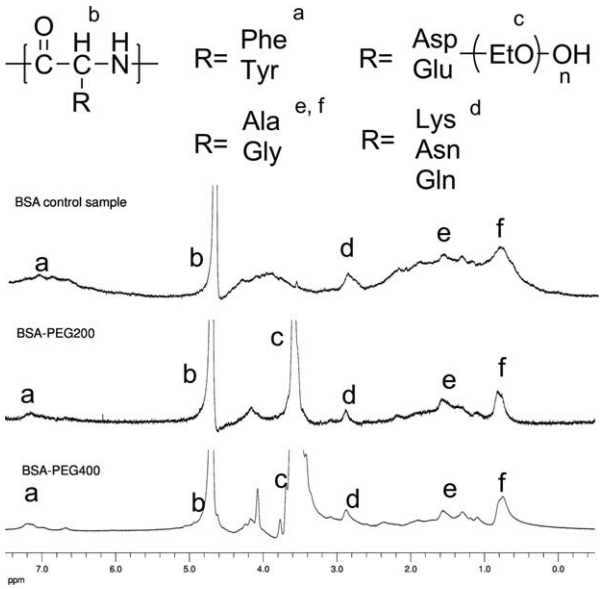

Figure 5. H[1]-NMR spectra of BSA–PEG200 and BSA–PEG400.

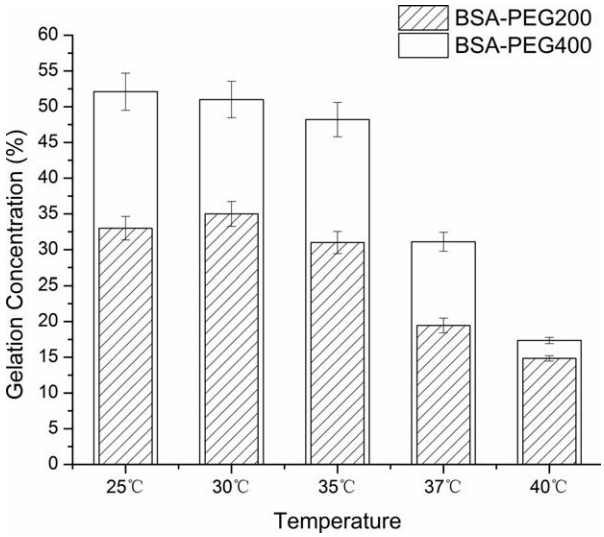

Figure 6. Temperature-dependent sol–gel transition concentration of BSA–PEG200 and BSA–PEG400.

was surprising to find a significant difference of the temperature and concentration dependent behavior of the BSA–PEG precursors relative to the molecular weight of PEG (Figure 6). At 30°C and below, fairly high sol–gel transition concentrations were observed: for BSA–PEG400 concentrations of over 50% and for BSA–PEG200 over 35% were necessary to form a gel. It seems that in the low molecular weight range of PEG (200 and 400) the impact of the chain length on the LCST does have a more pronounced effect than at longer chain lengths (MW > 3000 DA) as reported in other research.[40] Therefore, for BSA–PEG200 lower amounts of precursor were required for a gel to form than for BSA–PEG400. It could be argued that inter- and intramolecular hydrogen bonds usually supporting the BSA backbone structure, switch to intramolecular H-bonds with water upon PEGylation as has been hypothesized with PEG-grafted glutamates,[20] which would explain the water solubility of the grafted derivatives. This effect might be more pronounced the shorter the PEG molecular chain. Approaching the temperature range of 37–40°C, sol–gel transition concentrations considerably dropped and the difference between PEG200 and PEG400 almost disappeared; both hydrogels could be formed at a concentration of 15% at 40°C. Above 45°C the hydrogel precursors were unable to produce a gel. Instead, a slurry and finally, a brownish white precipitate formed.

At low precursor concentrations aggregate sizes were relatively small (Figure 7; approximately 200 nm in the case of BSA–PEG200) and almost spherical [Figure 8(a,b)]; larger agglomerates were formed with increasing concentration. The variation in shape and size was greater in the case of BSA–PEG400 [Figure 8(b)]. At 15% both BSA–PEG gels appeared to have similar aggregate sizes that were by about a factor of 10 larger than at 1% (Figure 7). In Figure 8(c), the TEM of the BSA–PEG200 precursor is displayed; upon heating to 40°C, the visual appearance of the gel corresponds to the one shown in Figure 1 (upper right hand corner).

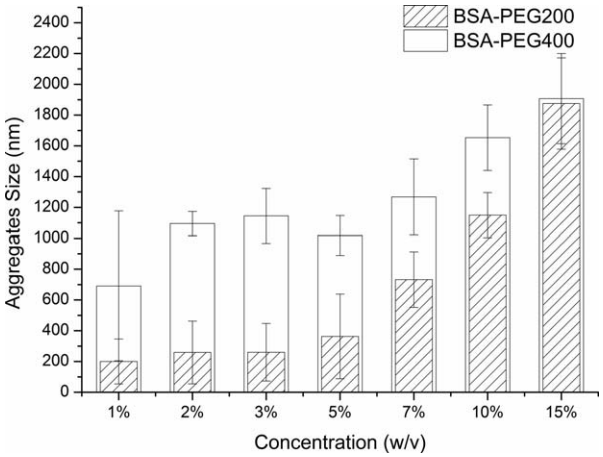

Figure 7. Particle size of BSA–PEG200 and BSA–PEG400 aggregates in 0.05*M* PBS (pH 7.40).

The morphology of the dried hydrogel was studied by scanning electron microscopy (SEM, Figure 9). The dry gels showed a structure with relatively large pores but seemed to be surprisingly compact after the water had been removed by lyophilization, leaving a BSA–PEG skeleton. Since water is the major constituent of a hydrogel, a more porous microarchitecture could have been expected.

A rheology study was performed to compare the viscoelastic behavior of the hydrogels and their precursors. The results are shown in Figure 10. The hydrogel precursors (delta symbols) showed a slight response at room temperature with low values for the storage (G') and loss modulus (G''). For both BSA–PEG200 and BSA–PEG400 hydrogels (square symbols) G' increased by a factor of approximately 10 and G'' by a factor of about 4 when gelation occurred after a 10-min heating period to 40°C. The hydrogels formed with a very low G' value (2 kPa) under the test conditions. The G'/G'' ratios for BSA–PEG200 and for BSA–PEG400 hydrogels were around 6–7 at 1 Hz frequency, which indicates that the hydrogel precursors transformed to materials of higher consistency.

Drug Delivery

Drug loading experiments were performed using 5-fluorouracil (5-FU), a common anticancer drug,[41] to illustrate that the capability of BSA–PEG gels to carry small drug molecules has been preserved, at least to a certain extent (Figure 11). Drug loading of 5-FU on to native BSA showed to follow a linear course; it

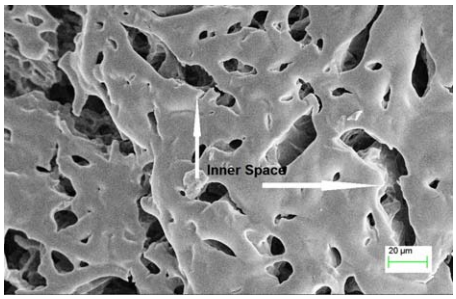

Figure 9. SEM image of dried BSA–PEG200 hydrogel with porous inner space. [Color figure can be viewed in the online issue, which is available at wileyonlinelibrary.com.]

was found to be lower by a factor of four for both BSA–PEG hydrogels compared to BSA, but also close to linear ($R^2 = 0.97$ for BSA–PEG200 and $R^2 = 0.90$ for BSA–PEG400). Mass spectra and H^1-NMR experiments had shown that PEG reacted with approximately one-fifth of the amino acid residues in BSA (Glu and Asp; Figures 3 and 5). Thus, it can be assumed that some of the amino acids responsible for interaction with 5-FU were occupied by PEG grafts. The difference in molecular weight of PEG proved to be insignificant in this case. However, it is important to state that the incorporation of 5-FU did not affect the sol–gel transition behavior of either BSA–PEG hydrogel.

The release profiles of 5-FU for BSA and BSA–PEG gels are shown in Figure 12. From both BSA–PEG200 and BSA–PEG400 less 5-FU was discharged into PBS buffer solution compared to native BSA. Both PEGylated hydrogels still contained almost 50% of the drug after 48 h exposure to the release medium, while the BSA control had liberated approximately 90% of the drug. Thus, although the PEGylated hydrogels could hold less of the drug overall (Figure 11), they initially freed a lower amount of 5-FU than BSA and therefore might be considered for future drug carrier applications with sustained release capabilities.

Biodegradation Studies

Biodegradation experiments *in vitro* of the hydrogels were conducted to evaluate their stability and degradability in PBS buffer solution at pH 8. From Figure 13, it can be seen, that both BSA–PEG200 and BSA–PEG400 hydrogels experienced a steady weight loss even without the addition of trypsin, a metabolizing enzyme; overall, after 144 h over 50% of the hydrogels were still left intact. It is likely that the BSA–PEG hydrogel aggregates

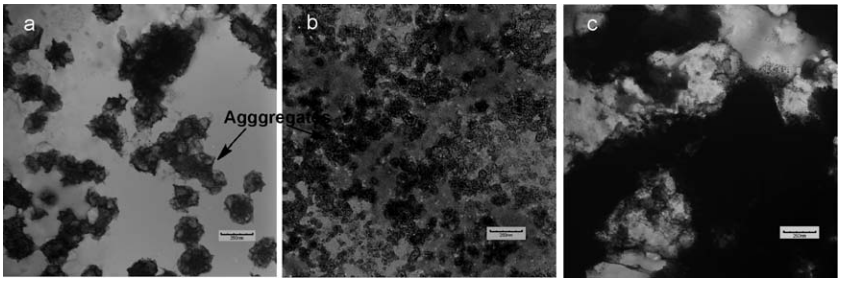

Figure 8. TEM images of (a) BSA–PEG200 aggregates at 1% in PBS; (b) BSA–PEG400 aggregates at 1% in PBS; (c) BSA–PEG200 aggregates at 15% in PBS.

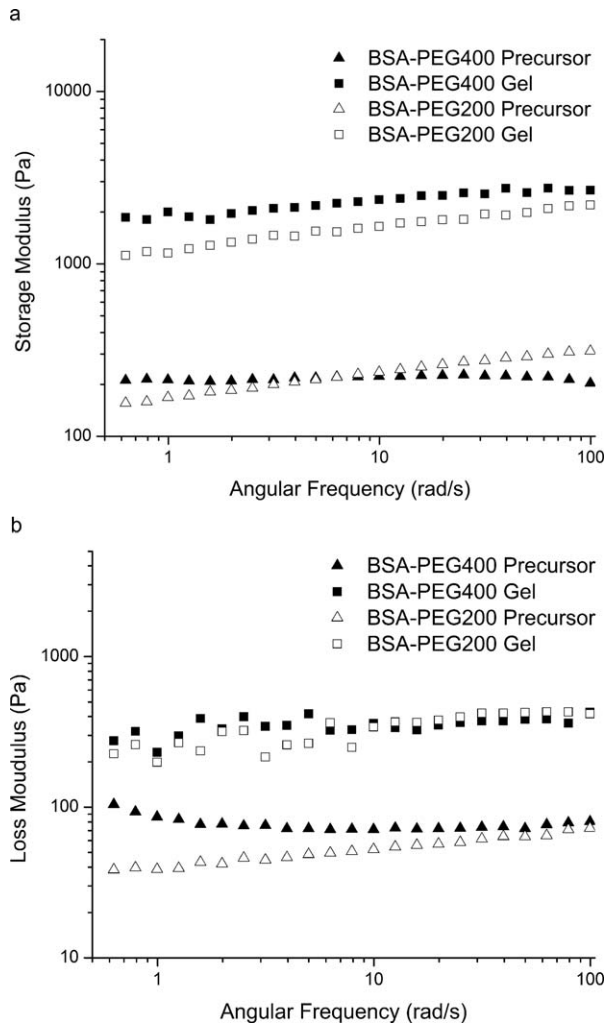

Figure 10. Rheologic properties of PEGylated BSA hydrogels and precursors: (a) storage modulus and (b) loss modulus.

slowly collapsed and disintegrated as the buffer solution eroded their three-dimensional arrangement. Trypsin clearly expedited the degradation of the hydrogels and led to rapid disintegration

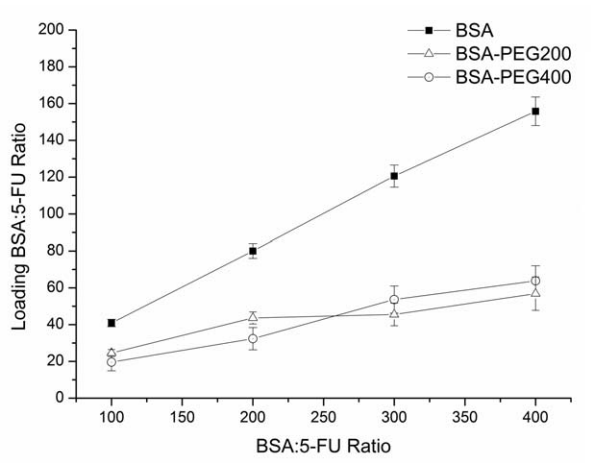

Figure 11. 5-FU loading profile on to BSA–PEG hydrogels and native BSA.

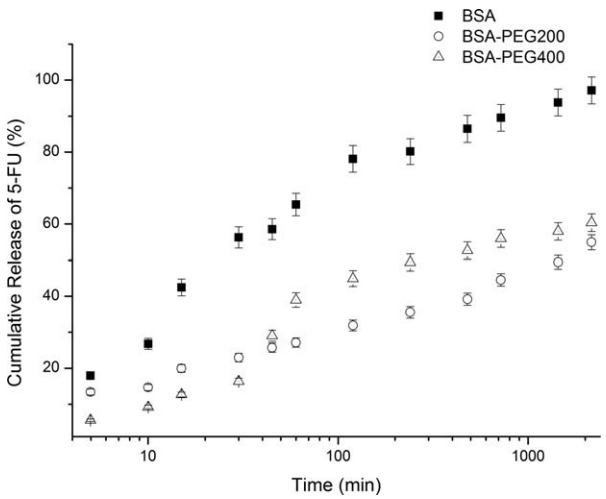

Figure 12. 5-FU discontinuous release profiles in 0.05*M* PBS at pH 7.4.

within less than 50 h, faster in the case of BSA–PEG400 than with BSA–PEG200. These observations indicate that modifying BSA with PEG grafts—though only to a fairly small extent and with just short graft lengths—led to enhanced hydrophilicity and susceptibility to biodegradation. These results could play an important role in drug delivery applications, where the drug was to be completely dispensed over a relatively short time frame.

CONCLUSIONS

In this work, a novel approach was introduced to synthesize a grafted BSA hydrogel via esterification of approximately one fifth of the acidic residues in BSA with PEG200 and PEG400, respectively. Grafting ratios of the BSA–PEG derivatives were determined by MALDI-TOF mass spectrometry and H^1-NMR spectroscopy. It was possible to form BSA–PEG hydrogels with interesting sol–gel transition behavior in the range of body temperature: with decreasing concentration and temperatures increasing from 25 to 37–40°C, small spherical precursor assemblies formed into larger aggregates within minutes. The sol–gel

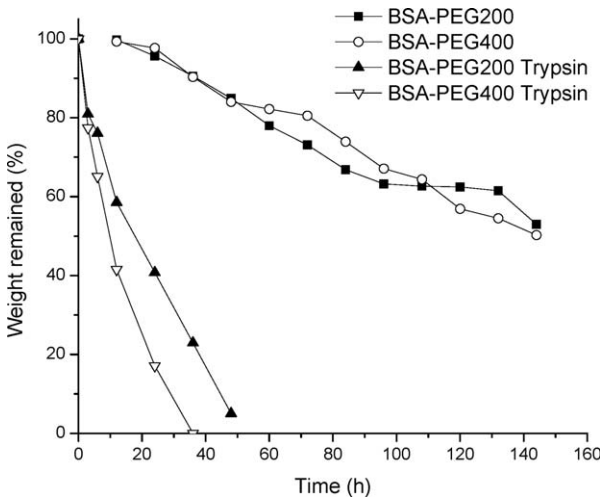

Figure 13. Biodegradation of BSA–PEG hydrogels at pH 8 without trypsin (square and round symbols) and with trypsin (triangular symbols).

transition concentration for both BSA–PEG200 and BSA–PEG400 hydrogels was 15%. The chain length of the PEG grafts only played a role in the lower concentration range and at temperatures less than 35°C. Due to the overall relatively low grafting ratios, the secondary and tertiary structure of BSA could be preserved in the BSA–PEG hydrogels. The hydrogels were capable of holding a small drug molecule, such as 5-FU. The release profile for 5-FU into buffer solution showed that the hydrogels could slow the release compared to native BSA. The hydrogels exhibited biodegradability, especially in the presence of a metabolizing enzyme. In future biomedical applications, BSA–PEG hydrogels could function as interesting drug delivery vehicles which, due to their sol–gel transition behavior, might even be considered for injectable alternatives. With the observed gelation conditions they might also perfectly fit the environment of a tumor (temperature slightly higher than normal body temperature) and the gels could provide a reservoir for sustained release of an anticancer drug.

ACKNOWLEDGMENTS

The author would like to thank Dr. Dongles Goodwin and Ms. Yu Wang for assistance with the CD spectra and Dr. Ramesh Jeganathan and Mr. Chen Zheng for assistance with the SDS-PAGE tests.

REFERENCES

1. Buwalda, S. J.; Boere, K. W.M.; Dijkstra, P. J.; Feijen, J.; Vermonden, T.; Hennink, W. E. *J. Control Release in press*, **2014**. DOI: 10.1016/j.jconrel.2014.03.052.
2. Yaszemski, M. J.; Trantolo, D. J.; Lewandrowski, K.-U.; Hasirci, V.; Altobelli, D. E.; Wise, D. L. Tissue Engineering and Novel Delivery Systems, Marcel Dekker: New York, **2004**.
3. Li, Y. L.; Rodrigues, J.; Tomas, H. *Chem. Soc. Rev.* **2012**, *41*, 2193.
4. Macaya, D.; Spector, M. *Biomed. Mater.* **2012**, *7*, 1.
5. Overstreet, D. J.; Dutta, D.; Stabenfeldt, S. E.; Vernon, B. L. *J. Polym. Sci. Part A: Polym. Phys.* **2012**, *50*, 881.
6. Park, M. H.; Joo, M. K.; Choi, B. G.; Jeong, B. *Acc. Chem. Res.* **2011**, *45*, 424.
7. Bawa, P.; Pillay, V.; Choonara, Y. E.; du Toit, L.C. *Biomed. Mater.* **2009**, *4*, 1.
8. Klouda, L.; Mikos, A. G. *Eur. J. Pharm. Biopharm.* **2008**, *68*, 34.
9. Teixeira, L. S.; Feijen, J.; van Blitterswijk, C. A.; Dijkstra, P.J.; Karperien, M. *Biomaterials* **2012**, *33*, 1281.
10. Schild, H. G. *Prog. Polym. Sci.* **1992**, *17*, 163.
11. Schmaljohann, D. *Adv. Drug Deliv. Rev.* **2006**, *58*, 1655.
12. Ward, M. A.; Georgiou, T. K. *Polymers* **2011**, *3*, 1215.
13. Hatefi, A.; Amsden, B. *J. Controlled Release* **2002**, *80*, 9.
14. Kan, P.; Lin, X. Z.; Hsieh, M. F.; Chang, K. Y. *J. Biomed. Mater. Res. Part B* **2005**, *75B*, 185.
15. Meenach, S. A.; Anderson, K. W.; Hilt, J. Z. *J. Polym. Sci. Part A* **2010**, *48*, 3229.
16. Yu, L.; Chang, G.; Zhang, H.; Ding, J. *J. Polym. Sci. Part A: Polym. Chem.* **2007**, *45*, 1122.
17. Alexander, A.; Ajazuddin, J.; Khan, S.; Saraf, S. *J. Controlled Release* **2013**, *172*, 715.
18. Luzon, M.; Boyer, C.; Peinado, C.; Corrales, T.; Whittaker, M. R.; Tao, L.; Davis, T. P. *J. Polym. Sci. Part A: Polym. Chem.* **2010**, *48*, 2783.
19. Hoare, T. R.; Kohane, D. S. *Polymer* **2008**, *49*, 1993.
20. Chen, C. Y.; Wang, Z. H.; Li, Z. B. *Biomacromolecules* **2011**, *12*, 2859.
21. Jonker, A. M.; Lowik, D.; van Hest, J. C. M. *Chem. Mater.* **2012**, *24*, 759.
22. Oss-Ronen, L.; Seliktar, D. *Acta Biomater.* **2011**, *7*, 163.
23. Pahimanolis, N.; Sorvari, A.; Dang Luong, N., Seppälä, J. *Carbohydr. Polym.* **2014**, *102*, 637.
24. D'Este, M.; Alini, M.; Eglin, D. *Carbohydr. Polym.* **2014**, *90*, 1378.
25. Chen, T.; Embree, H. D.; Brown, E. M.; Taylor, M. M.; Payne, G. F. *Biomaterials* **2003**, *24*, 2831.
26. Abuchowski, A.; Vanes, T.; Palczuk, N. C.; Davis, F. F. *J. Biol. Chem.* **1977**, *252*, 3578.
27. Gayet, J. C.; Fortier, G. *J Controlled Release* **1996**, *38*, 177.
28. Castelletto, V.; Krysmann, M.; Kelarakis, A.; Jauregi, P. *Biomacromolecules* **2007**, *8*, 2244.
29. Plesner, B.; Fee, C. J.; Westh, P.; Nielsen, A. D. *Eur. J. Pharm. Biopharm.* **2011**, *79*, 399.
30. Shakya, A. K.; Sami, H.; Srivastava, A.; Kumar, A. *Prog. Polym. Sci.* **2010**, *35*, 459.
31. Hamley, I. W.; Krysmann, M. *J. Langmuir* **2008**, *24*, 8210.
32. Zarafshani, Z.; Obata, T.; Lutz, J. F. *Biomacromolecules* **2010**, *11*, 2130.
33. Veronese, F. M.; Pasut, G. *Drug Discov Today* **2005**, *10*, 1451.
34. Elstad, N. L.; Fowers, K. D. *Adv. Drug Deliv. Rev.* **2009**, *61*, 785.
35. Lin, Z.; Gao, W.; Hu, H.; Ma, K.; He, B.; Dai, W.; Wang, X.; Wang, J.; Zhang, X.; Zhang, Q. *J Controlled Release* **2014**, *174*, 161.
36. Li, X. Y.; Li, T. H.; Guo, J. S.; Wei, Y.; Jing, X. B.; Chen, X. S.; Huang, Y. B. *Biotechnol. Prog.* **2012**, *28*, 856.
37. Kelly, S. M.; Jess, T. J.; Price, N. C. *Biochim. Biophys. Acta* **2005**, *1751*, 119.
38. Wu, Y.; Wang, K.; Buschle-Diller, G.; Liles, M. R. *J Appl. Polym. Sci.* **2013**, *129*, 3591.
39. Barone, G.; Giancola, C.; Verdoliva, A. *Thermochim. Acta* **1992**, *199*, 197.
40. Lutz, J.-F.; Hoth, A. *Macromolecules* **2005**, *39*, 893.
41. Hedley, D.; Ogilvie, L.; Springer, C. *Nat. Rev. Cancer* **2007**, *7*, 870.